J Mater Sci (2012) 47:7356–7366
DOI 10.1007/s10853-012-6551-7

FIRST PRINCIPLES COMPUTATIONS

First principles calculations of H-storage in sorption materials

Abhishek Kumar Singh · Boris I. Yakobson

Received: 23 January 2012 / Accepted: 3 May 2012 / Published online: 24 May 2012

Abstract A review of various contributions of first principles calculations in the area of hydrogen storage, particularly for the carbon-based sorption materials, is presented. Carbon-based sorption materials are considered as promising hydrogen storage media due to their light weight and large surface area. Depending upon the hybridization state of carbon, these materials can bind the hydrogen via various mechanisms, including physisorption, Kubas and chemical bonding. While attractive binding energy range of Kubas bonding has led to design of several promising storage systems, in reality the experiments remain very few due to materials design challenges that are yet to be overcome. Finally, we will discuss the spillover process, which deals with the catalytic chemisorption of hydrogen, and arguably is the most promising approach for reversibly storing hydrogen under ambient conditions.

Introduction

Hydrogen is the most abundant element in the universe. It is a carrier of clean and renewable energy and is considered as a potential major alternative to fossil fuels [1, 2]. The fossil fuels such as oil, coal, and natural gases produce green house gases, which have a long-lasting effect on our environment. On the other hand, hydrogen is clean, non-toxic, contains more energy per unit mass than any other fuel, and produces water as byproduct. One of the biggest hurdles to its practical usage is a lack of storage media, which could meet the US Department of Energy's 2015 targets [3], i.e., gravimetric $g > 5.5$ wt% and volumetric $v > 40$ kg/m^3 (to appreciate the challenge, this is greater than half-density of 71 kg/m^3 of liquid hydrogen, at 20 K). This stringent requirement fueled an extensive search for materials, which can store hydrogen within a reasonable volume without significant increase in weight, essentially they must be composed of elements lighter than Al. In addition, an efficient storage media should be able to adsorb/desorb H_2, reversibly and repeatedly within the achievable temperatures and pressures. This condition restricts the Hydrogen adsorption energy in a storage media to a range of $\sim$0.1–0.5 eV/H_2. To find a storage media which meets these two requirements simultaneously is one of the most challenging problems for hydrogen economy. Among various possibilities, the carbon-based adsorbents [4–9] are recognized as strong candidates for storage media as the large surface area and lighter weight make the required volumetric and gravimetric content possible, while considerable abundance of carbon allotropes suggests economic feasibility. Moreover, owing to their ability to bind hydrogen both by physisorption and chemisorptions, graphitic structures can satisfy required binding energy criterion.

Kubas bonding

An extensive search for efficient hydrogen storage materials led to finding of several promising candidates

A. K. Singh (✉)
Materials Research Centre, Indian Institute of Science, Bangalore 560012, India
e-mail: abhishek@mrc.iisc.ernet.in

B. I. Yakobson
Department of Mechanical Engineering and Materials Science, Rice University, Houston, TX 77005, USA

B. I. Yakobson
Department of Chemistry, Rice University, Houston, TX 77005, USA

including metal hydrides [10–12], graphitic sorption nanomaterials [4, 7], and metal organic frameworks (MOF) [13, 14]. Although promising, these individual storage materials suffer from one or other forms of practical difficulties, e.g., too strong metal-H binding in metal hydrides often results into poor kinetics, whereas too weakly physisorbed H_2 in graphitic nanostructures require storage at very low temperature. Between strong chemisorption and weak physisorption there exists Kubas [15] type of interaction—a "non-classical" form of binding of H_2 to metal with a binding energy of $\sim$0.4 eV/H_2—which is ideal for the reversible storage at ambient conditions. A single metal atom can bind multiple H_2 molecules [15, 16] via Kubas interaction leading to high gravimetric and volumetric density.

Chemistry of Kubas bonding

Kubas interaction [15], is based on Lewis concept of donation of electron pairs. In such complex, a σ-bonding electron pair (H:H) of H_2 molecule interacts with the *d* orbital of a metal via electron donation. The uniqueness in the stabilization of M–H_2 complex is backdonation (BD), i.e., the retrodative donation of electrons from a filled metal *d* orbital to the σ^* orbital of H–H bond. The BD is an important process in adding and orienting the H_2 side-on to metal as well as in activating the dissociation of H–H bond. If the backdonation becomes too strong, it leads to over-population of σ^* orbital and results into breaking of H–H bond and eventually leads to a strong M–H bonding as in metal hydride. On the other hand, a balance of BD and σ donation stabilizes the Kubas complexes. The H–H bond length, d_{HH}, is stretched about 15–25 % over its value in free H_2 (0.74 Å). The d_{HH} is controlled by the ability of metal to backdonate electrons; therefore, varies with the change of metal atoms.

Kubas bonding and H_2 storage

Historically, Niu et al. [16] have shown, for the first time, using first principle calculations that while a neutral Ni atom can bind only two dissociated hydrogen atoms, a Ni^+ cation can bind up to six hydrogen molecules (dihydrogen) with a binding energy of about 0.4 eV/H_2. Gagligardi and Pyykko [17] extended this study to include other transition metal atoms and have shown that Ti, Cr, Mo, W, and Mn can also adsorb more than 10 dihydrogen molecules. These two studies were focused on estimating the H_2 adsorption capacity of single TM atom in vacuum, which was not very attractive for practical application due to the clustering problem of exposed metal atoms. The deadlock was broken by two groups around the same time, Yildrim et al. [18] and the Zhang and coworkers [19] who proposed an entirely new concept to utilize this phenomenon to design path-breaking organometallic molecules based on transition metal-decorated carbon nanotube and fullerene C_{60} as storage system, Figs. 1 and 2, respectively. They used first principles calculations and show that these organometallic molecules can reversibly store up to 9 wt% hydrogen, at room temperature and near ambient pressure. Zhang and coworkers [19] exploited the fact that H_2 and cyclopentadiene (Cp = C_5H_5) rings can be ligands for TMs. A TM atom interacts with a Cp ring through Dewar coordination [20] and with a dihydrogen ligand through a Kubas interaction [21]. While these two types of bondings are of historical importance in coordination chemistry [9, 10], Zhao et al. [19] were the first to propose an idea of joining the two in designing a solution for hydrogen storage media. They show that a Cp[ScH_2] complex can store 6.7 wt% of dihydrogen. This approach has a small practical problem as after

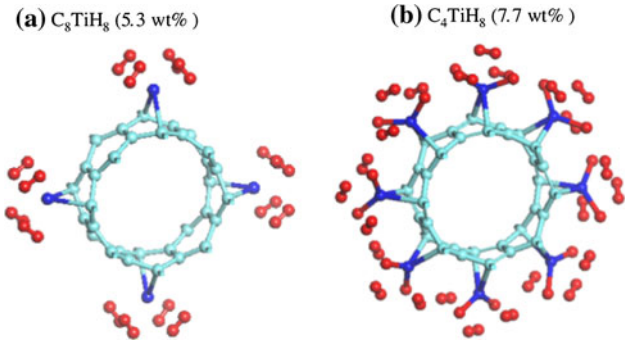

Fig. 1 The structure of high-density hydrogen covered Ti-coated (8,0) nanotube. The two structures have different concentration of metal atoms. The *figure* is reproduced from the Ref. [18]

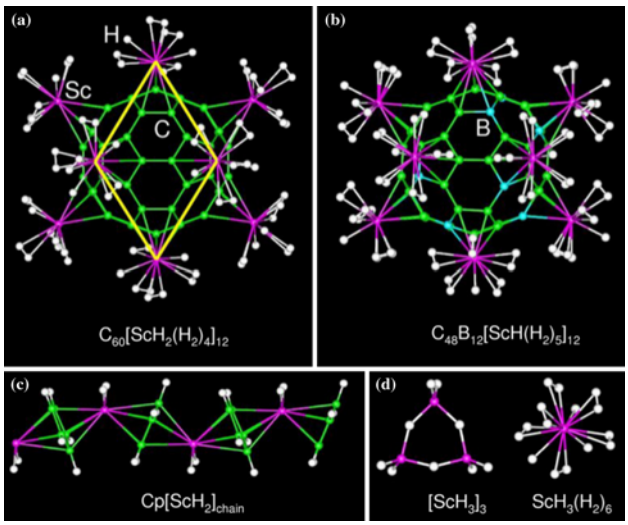

Fig. 2 Optimized structures of various transition metal atom-decorated fullerenes with the full hydrogen coverage, **a** $C_{60}[ScH_2(H_2)_4]_{12}$, **b** $C_{48}B_{12}[ScH(H_2)_5]_{12}$, **c** $Cp[ScH_2]_{chain}$, and **d** $[ScH_3]_3$ (*left*) and $ScH_3(H_2)_6$ (*right*). For clarity, only part of the buckyballs is shown. The *figure* is reproduced from the Ref. [19]

desorption of hydrogen these complexes may polymerize, which can make this process irreversible. In order to overcome this limitation, they show that these complexes can be arranged symmetrically on a buckyball, species such as $C_{60}[ScH_2]_{12}$ and $C_{48}B_{12}[ScH]_{12}$. These metal-decorated fullerenes were found to be stable and could reversibly adsorb additional hydrogen, resulting in capacities of 7.0 and 8.77 wt%, respectively, as shown in Fig. 2. As expected from such Kubas complexes, the binding energy was found to be ideal for vehicular applications, 0.3–0.4 eV. Further support to this idea was lent by experimental synthesis of TM-coated buckyballs [22] and nanotubes [23].

A comprehensive study on Ti-decorated carbon nanotubes were carried out by Yildrim et al. [18]. They show that Ti-decorated CNTs are stable structures, Fig. 1. A detailed study on the four armchair (n,n) ($n = 4$, 5, 6, and 7) and five zigzag (n,0) ($n = 7$, 8, 9, 10, 11, and 12) nanotubes, revealed the dependence of binding of metal atoms on CNTs, upon their chiralities and curvatures. Furthermore, they concluded that a single Ti atom absorbed on hexagons of SWNT could bind up to four dihydrogen molecules. This was observed to be a general behavior in a very large number of nanotubes and in other carbon-based nanoclusters, including C_{60} [24]. They studied the effect of Ti concentration by covering ¼ and ½ of the hexagons on the nanotubes by Ti atoms and found that in this configuration the system stores 5 to 8 wt% of H_2. Furthermore, the binding energies were in the range of 0.43 to 0.50 eV/H_2, which was close to the required value for a reversible storage. They extended their study to C_{60} decorated by the first row TM atoms, including Sc, Ti, V, Cr, Mn, and Fe atoms [24]. The different transition metal atoms get adsorbed at different sites. For example, Sc and Ti prefer the hexagonal site, while V and Cr prefer the double bond sites. Heavier metals such as Mn, Fe, and Co do not bind to C [24]. Each metal atom can adsorb up to four dihydrogen molecules with an average binding energy of 0.3–0.4 eV/H [24]. Furthermore, they report that systems with high metal coverage can adsorb up to 56 H_2 molecules corresponding to 7.5 wt%.

Lighter metal atoms as adsorbents

Owing to advantage of wt%, lighter metal atoms [25–27] were also explored as a multiple dihydrogen molecule adsorbent. Jena and coworkers [25] have shown that an isolated Li-decorated C_{60} cluster—where Li atoms are capped onto the pentagonal faces of the fullerene—is very stable and can store up to 120 hydrogen atoms in molecular form with an average binding energy of 0.075 eV/H_2. Yoon et al. [27] introduce a new concept of polarization field, which is caused by the adsorption of Ca atom on the surface of fullerene, acts as attractor for the H_2 molecules. The binding strength dependence on the type of metal atoms, e.g., while Be and Mg bind weakly, Ca, and Sr can be adsorbed strongly on C_{60}, with preference for a monolayer coating. The strong binding for Ca and Sr is attributed to the charge transfer to the empty d levels of the metals. They argue that the charge redistribution gives rise to electric fields surrounding the coated fullerenes, which function as effective molecular hydrogen attractors. They report hydrogen uptake in such materials in excess of 8.4 wt%. Kim et al. [26] have explored the possibility of lighter atom impurity doping of C_{36} and reported enhancement of storage capacity. They have observed Li and F prefer to be at interstitial site while N, B, and Be, prefer substitutional sites. However, only Be and B show significant adsorption energy 0.39 and 0.65 eV/H_2, respectively. Their analysis show that a strongly localized, empty p_z orbital of B and Be is essential for the enhanced interaction with the occupied σ orbital of H_2, which leads to partial charge transfer from H_2 to the fullerene. A room temperature reversible storage capacity of 1.7 wt% is reported for $C_{54}Be_6$ with adequate binding energies for reversible adsorption.

These works led to a great interest in this technologically important area of research. Several interesting possibilities and designs have been proposed. For example, TM-ethylene complexes are once shown to store as much hydrogen [28, 29] as 14 wt%. Very recently, Sorokin et al. [30] have demonstrated that hydrogen adsorption on calcium-decorated carbyne chain by ab initio density-functional calculations. The estimation of surface area of carbyne gives the value four times larger than that of graphene, which makes carbyne attractive as a storage scaffold medium. Furthermore, calculations show that a Ca-decorated carbyne can adsorb up to 6 H_2 molecules per Ca atom with a binding energy of <0.2 eV, desirable for reversible storage, and the hydrogen storage capacity can exceed 8 wt%. DFT was the most reliable working horse for all these works.

Clustering of metal atoms

These materials are promising and, if experimentally realized, can easily meet the material-based DOE targets [3] for 2015. The biggest hurdle on the way to success of such materials is the tendency of metal atoms to aggregate [31, 32]. In order to prevent the clustering of metal atoms, the doping of carbon nanostructures by boron has been proposed [19]. Owing to stronger B–TM binding, boron acts as an anchor to the metal atom and prevents the clustering. However, the practical difficulty of doping carbon nanostructures with boron remains a challenge for successful synthesis of such materials. Despite attractive binding energy and sound design proposed by DFT calculations,

experiments were not able to catch up with the theoretical work. There has been enormous effort to reproduce these results experimentally; however, it remains hard to match the predicted fantastic values of the wt% till today.

An early indication of the possible cause of this problem comes from the work of Sun et al. [31], where they show that a 12 atom cluster of Ti is energetically more favorable than isolated Ti atoms decorating the surface of C_{60}. This would essentially translate into a much lower wt% on such system. Krasnov et al. [32] carried out a detailed study to address the important questions on energetics, kinetics of metal aggregation, and the hydrogen uptake on the aggregated metal clusters. They studied the aggregation mechanism of Sc atoms on the surface of carbon nanotubes and graphene. They performed a systematic study to estimate the binding strength between a single Sc atom and the SWNT and its dependence on the diameter and chirality angle, Fig. 3. A wide range of zigzag-type SWNTs with diameters ranging from 0.31 to 0.78 nm [(m,0) where $m = 4, 5,\ldots, 10$] and SWNTs with chirality angles from 0 to 30° [(n,8 − n), where $n = 4, 5,\ldots, 8$]) were considered [32], Fig. 3. The binding energy of a single Sc on small diameter SWNT is very strong (e.g., 3.37 eV on (4,0) SWNT), but decreases fast with increasing tube diameter (e.g., decrease to 1.83 eV on (10,0) SWNT), Fig. 3. This is attributed to the decrease in chemical reactivity of the nanotubes with decreasing curvature as the hybridization approaches closer to sp^2. On the other hand, the binding energy of a Sc atom on graphene, which represents a limiting case of large diameter SWNT, is only 0.2 eV. Their results show a very strong dependence of binding energies on the diameter and chirality angle of SWNT. Although SWNTs with very small diameters bind Sc atoms strongly, binding energy remains sensitive to the tube chirality angle and tube type and decreases fast with increasing SWNT diameter. For SWNTs of 1–2 nm, the binding energy predicted to be significantly lower of the order of 1 eV/atom. Compared to the 3.90 eV/atom cohesive energy of Sc bulk [33], such a binding energy is too weak to prevent the Sc atoms from aggregation.

Kinetic possibility of aggregation was examined by evaluating the migration barrier of Sc atom on the (4,0) nanotube along two symmetrically non-equivalent directions and reported to be 0.48 and 0.61 eV, respectively, Fig. 4. However, on the graphene, the migration barrier was only 0.15 eV. Among all the SWNTs studied there, (4,0) SWNT and graphene bind Sc atom most strongly and weakly, respectively. This has led to the conclusion that the diffusion barrier, E^*, of a single Sc atom on larger diameter SWNT surfaces will be less than that on (4,0) SWNT and higher than that on graphene and will lie in the range 0.15–0.48 eV. The diffusion frequencies were also estimated for these two extreme cases at room temperature

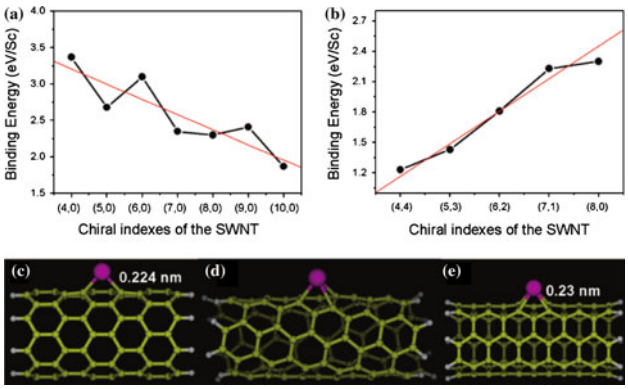

Fig. 3 Plots of **a** diameter and **b** chiral angle dependence of binding energies of a single Sc atom-decorated SWNTs. *Red lines* are the best linear fit of the energies. **c–e** are the optimized structures of Sc@(8,0), (6,2), and (4,4) SWNTs. The *figure* is reproduced from the Ref. [32] (Color figure online)

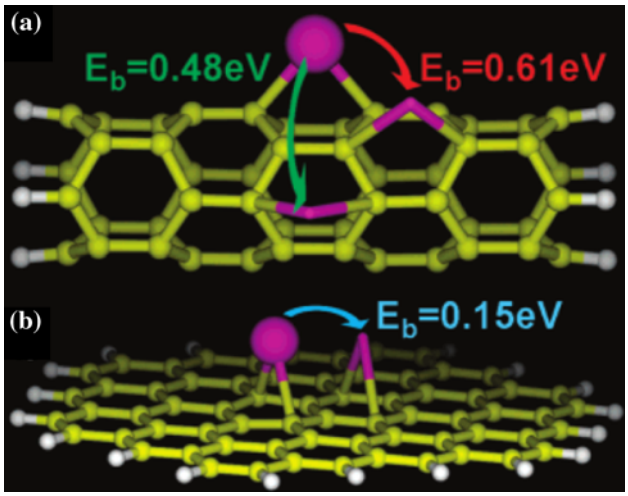

Fig. 4 Possible paths and barrier of Sc diffusion along SWNT (4,0) (*up*) and graphene layer (*down*) and corresponding barriers. The *figure* is reproduced from the Ref. [32]

($T = 298$ K) by transition state theory. The calculated diffusion frequency in this energy range was found to be $\sim 10^5$–10^{10} s^{-1}, implying that the single Sc atoms would be extremely mobile on both SWNT and graphene. From these analyses, it was concluded that aggregation of Sc on SWNT is both energetically and kinetically probable. Importantly, they also found that most of the adsorbed H_2 on the Sc_4 cluster were dissociated with much more stronger binding energies compared with Kubas type of binding, making desorption very hard at ambient conditions.

Design of new class of materials

The key to the success of hydrogen storage via Kubas interaction may lie in finding nanomaterials, where the

metal atoms are among the constituent elements (and thus cannot aggregate), yet retain their H-binding ability. One such class is metallacarboranes [34], derived from the carboranes, one of the most studied classes of boron clusters. Carboranes are essentially borane clusters containing one or more carbon atoms. Replacing one or more BH units of carboranes by metal atoms leads to formation of metallacarboranes. The advantage of having both metal and C in the same cage has been utilized in various applications, including even nanomotors [35].

Singh et al. [36] investigated hydrogen storage capacity of metallacarborane-based MOF, which was motivated by the experimental demonstration of 2 wt% of H_2 at 77 K via physisorption [37, 38] in icosahedral carborane-based MOF. Singh et al. [36] proposed and showed by density-functional theory calculations that metal in metallacarboranes can bind multiple hydrogen molecules, while carbon can link the clusters to form three-dimensional frameworks, Fig. 5. Replacing carboranes in MOF by metallacarboranes enhances the wt% due to adsorption of additional H_2 on metal atoms via Kubas interaction. This leads to storage of up to 8.8 wt% in metallacarbornes. Moving from a pure physisorption to Kubas type of H_2 binding increases the binding strength, which can insure room temperature storage. The binding energies lie within the reversible adsorption range at ambient conditions. Sc and Ti are recognized as the most optimal metals in maximizing the storage capacity. Furthermore, they show that carboxylate-based connectors have no effect on number of adsorbed H_2 molecules. Therefore, in addition to adsorbing H_2 via Kubas interaction, such frameworks will also physisorb H_2 in the pores, Fig. 5. Given the recent progress made in the carborane-based MOFs and abundance of metallacarboranes, such materials can soon become experimental reality.

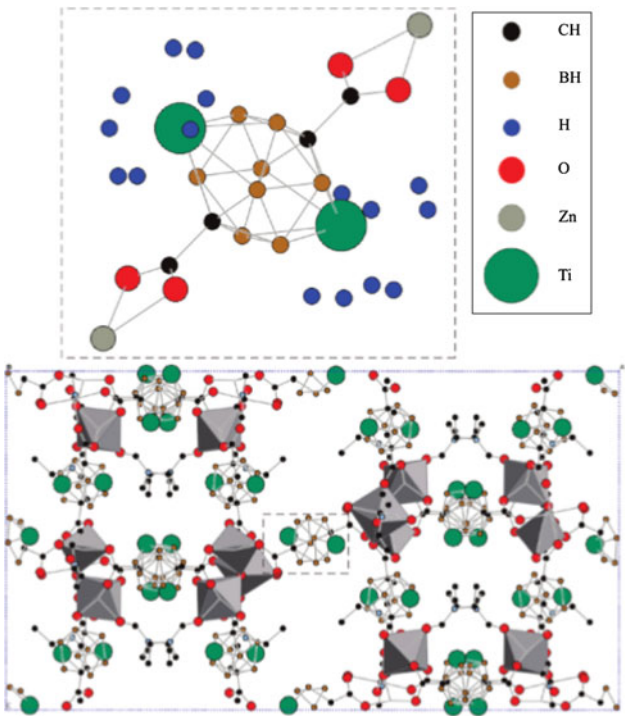

Fig. 5 Optimized structure of 1-5-$C_2B_8H_{10}Ti_2$ with the Zn-carboxylate groups attached. *Lower* likely structure of a MOF with 1-5-$C_2B_8H_{10}Ti_2$ linkers. The *figure* is reproduced from the Ref. [36]

Anchoring TM atoms onto some well-selected media has emerged as another promising approach to exploit Kubas type of binding. This has been explored both experimentally [39–42] and computationally [43, 44]. Hoang et al. [41] show that low coordinated V centers in vanadium hydrazide gels act as the Kubas H_2 binding sites. Hamed et al. [39] have shown the hydrogen storage capacity of mesoporous silica using tri- and tetrabenzyl Ti precursors. They reported up to 1.66 wt% storage, which was equivalent to an average of 2.7 H_2 per Ti center [39]. Vittilio et al. [42] used the IR spectroscopy to study the role of open metal atom sites in increasing H_2 adsorption in MOFs. These experiments are very encouraging as they show significant improvement in binding energies due to exposed metal sites [39–42], which are prohibited to cluster due to a novel architecture. Shevlin and Guo [43] proposed by density-functional theory that the native defects in CNT can enhance the Ti–CNT interaction and thereby reducing the chance of agglomeration. Similar to experimental work on silica, Wang et al. [44] showed interesting possibility of decorating graphene oxide (GO) by Ti. The Ti binds with the oxygen very strongly and thus reduces the chance of clustering.

Validity of DFT

A shadow of doubt has been cast over the reality of H_2 storage using Ca as decorative material. Cha et al. [45] have found that DFT for hydrogen adsorption geometry and binding energy is not consistent with the MP2 and CCSD(T) for the Ca^{1+} system. They show that the geometry of the four H_2 molecules adsorbed onto Ca^{1+} is only locally stable and energetically unstable in the MP2 and CCSD(T) results, whereas their DFT results show that the adsorption geometry of the four H_2 molecules is the global energy minimum. They also reported that this inconsistency exists not only in the case of the bare Ca^{1+} but also in the previously suggested potential hydrogen storage media such as Ca-adsorbed nanostructures. This work found further support by a similar study carried out by Bajdich et al. [46] by means of quantum Monte Carlo simulations of the binding of single and quadruple hydrogen molecules on a positively charged Ca ion. They show that unlike DFT, single determinant QMC calculations find no binding at short range by approximately 0.1 eV for the quadruple

hydrogen molecule case for a fixed hydrogen bond length of 0.77 Å. They furthermore show the differences in density-functional calculations using common functionals (LDA and B3LYP) and QMC binding curve. They found that use of full Hartree–Fock exchange and Perdew–Burke–Ernzerhof (PBE) correlation (HFX + PBEC) obtains close agreement with the QMC results, both qualitatively and quantitatively.

Contrary to the above finding, Sun et al. [47] performed highly accurate calculations by the MP2 perturbation theory and coupled cluster theory with single, double, and perturbative triple excitations for the dihydrogen binding on four representative systems that cover a wide range of sorbent materials including Ca. They carried out a thorough comparison with nine widely used density-functional theory exchange—correlation functionals and found that the PBE and PW91 results are accurate to within a few hundredths of an eV/H_2. They claim to validate the predictions obtained by these methods [47]. The reasons for discrepancy between these two works could be the use of Ca^{1+} as a model for the Ca, which decorate graphitic material. The exact charge transfer from Ca to the graphitic material is definitely not an integer +1 as assumed by Cha et al. [45]. Furthermore, Bajdich et al. [46] do not allow relaxation of the system, which is a key to stabilization of dihydrogen binding. For the case of TM, the dihydrogen binding is a reality beyond any doubts; however, for Ca atom, more experiments are required to settle this issue.

Chemisorption (spillover)

As discussed in the previous section, the H-storage capacity of sp^2-carbon materials (e.g., graphene, nanotubes, fullerenes, and nanofibers) can be significantly enhanced by decorating them with metal atoms [18, 19, 24, 29, 48, 49]. On the other hand, the tendency of metal atoms to aggregate and cluster [31, 32], presents biggest challenge, which has yet to be overcome in a satisfactory way. Recently, a new role for these clustered metal atoms is revealed, where they act as catalyst and enhance the hydrogen uptake of substrates via spillover [50–53]. In the spillover process, the H_2 molecules dissociate at metal catalyst; the atomic H then binds to the receptor-substrate, which otherwise (without the catalyst) would not adsorb hydrogen [54]. It is empirically established that the spillover can further be enhanced by adding bridges [55] between the catalyst and receptor. Significant enhancement has been reported in hydrogen storage via spillover on CNTs [50, 52, 55–65], carbon fibers [53, 62, 66–70], activated carbons and templated carbons [71–76], MOFs [77–81], and COFs [82]. The most widely used catalysts for spillover of H-atoms on graphitic materials are Pd, Pt, and *3d*-transition metal atoms. On the other hand, the best coverage of H on graphitic substrates can be achieved when they are hydrogenated from both sides, and spillover [83] is considered as possible path to achieving it. Such fully hydrogenated graphene would have stoichiometry CH, with 7.7 wt% of hydrogen [84–86], meeting the DOE goals. The theoretical saturation spillover storage capacities for different MOFs and COF-1 were calculated by Ganz and coworkers [87] by accurate ab initio quantum chemistry calculations. Their results show the theoretical capacities of 4.5 wt% for IRMOF-1, 5.7 wt% for IRMOF-15, and IRMOF-16. These studies further confirmed the applicability of hydrogen spillover to hydrogen storage.

Route for chemisorption of H on graphene

Even though spillover [54] has emerged as promising process to store hydrogen in graphitic materials under ambient conditions, fundamental question that how would an H-atom bind to graphene if it is more favorable for it to form H_2, however, was not well answered. Lin et al. [86] attempted to understand the process of spillover. They proposed hydrogen storage via spillover as phase nucleation process of full hydrogenation of graphene. They studied the hydrogenation of graphene by density-functional theory and found a tendency of clustering in adsorbed H-atoms. They computed the binding energy of such cluster of n hydrogen atoms defined as $\varepsilon_b(n) = (\mathrm{Eg} + n\varepsilon_H - E_{nH@g})/n$, where Eg, ε_H and $E_{nH@g}$ are the energies of graphene, a single H-atom, and the total energy of hydrogenated graphene, respectively. The first hydrogen atom binds very weakly with the BE 1.5 eV less than of H_2, and therefore was not sufficient to initialize the spillover. The weak binding is due to breaking of the π bond between neighboring C atoms, (so-called starred and unstarred C, respectively) and leaving energetically unfavorable radical on one of the carbon atom. Next, H prefers to bind to this radical and lowers the energy, Fig. 6. The chemisorption of H changes the hybridization of the host C atom from sp^2 to sp^3 and the hydrogenated C atom buckles off the plane. If two adjacent C atoms are hydrogenated from the opposite sides, the induced strains compensate each other reducing the energy. Such configuration was found to be more stable than the one with both H's attached on the same side. The resulting BE remains weaker by 0.6 eV compared with the H_2.

Figure 6 shows BE for a series of structures and display the steady increase from 0.79 eV for a single H to 1.70 eV/H for a pair, to 2.16 eV/H for a sextet, and further to 2.35 eV/H for 24 adsorbed atoms, which already is 0.05 eV/H more than 1/2 E_{H2}. Finally, for a fully both-sided hydrogenated graphene of composition CH, the binding energy reaches 2.54 eV/H, exceeding 1/2 E_{H2} by

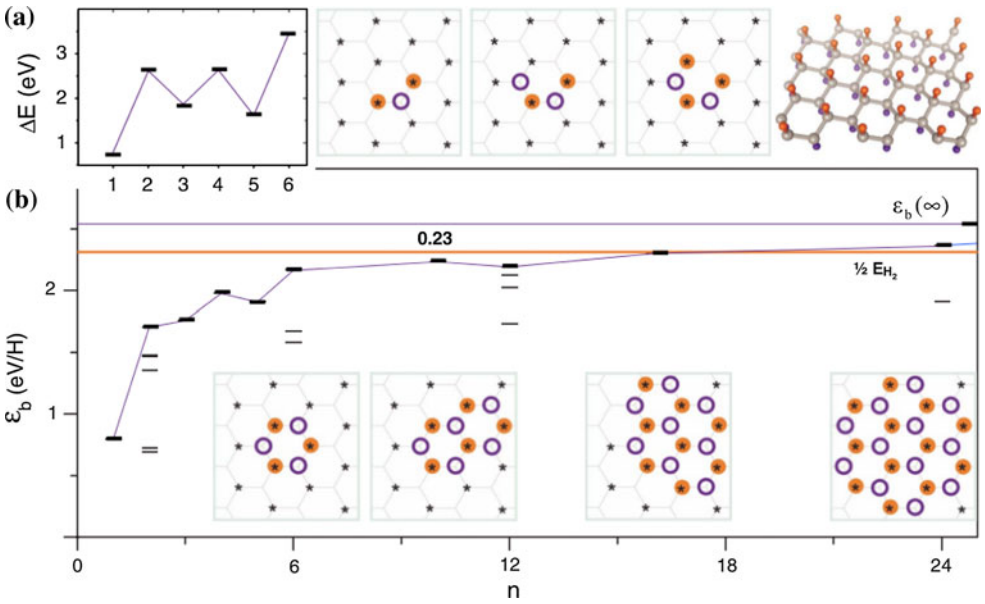

Fig. 6 The energy increment ΔE_n due to nth atom sorption versus its number (**a**). In **b**, binding energy per H for all clusters considered as a function of their size n. The *insets* show 3, 4, and 5 adsorbed H-atoms, followed by the infinite fully hydrogenated graphene. **b** The *thin line* connects the most stable configurations to guide the eye. The *insets* show the larger closed-ring structures with 6, 10, 16, and 24 atoms. The *figure* is reproduced from the Ref. [86]

0.23 eV/H. Clear minimum observed for configurations composed of six rings (e.g., of 6H, 10H, 16H, and 24H) have stronger binding than any others with incomplete six rings. A clear tendency of clustering was observed. Furthermore, the total energy fits well a continuum model of an island, which was decomposed into bulk and surface (island boundary) contribution, Fig. 7. For any given P and T, Gibbs formation energy $\Delta G^{P,T}(n)$ exhibit typical phase nucleation dependencies with the nucleation barrier ΔG^* and the critical size n^* (or l^*), where n and l are the number of adsorbed hydrogen and perimeter of the island, respectively. Most importantly, it was shown that the balance between the gas phase and storage phase can be changed reversibly by altering P and T closer to the ambient conditions, meeting the requirement for reversible storage, Fig. 7. This was the first time when first principles calculations resolved the controversy surrounded around the spillover process.

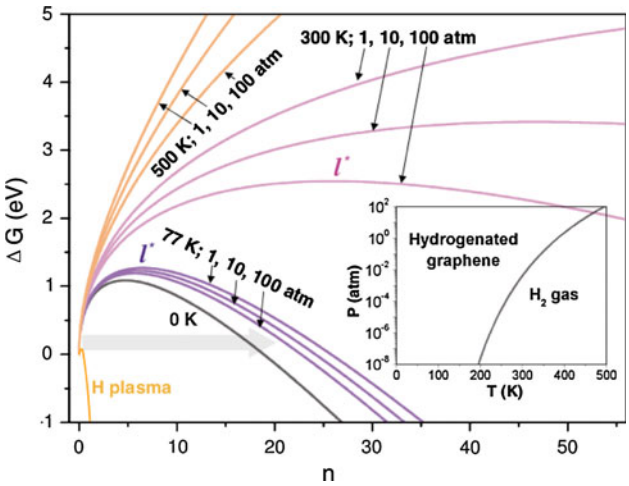

Fig. 7 Gibbs free energy of formation of a CH island in the graphene as a function of number of H, computed for different P and T. The typical nucleation-type shapes are characterized by the critical nucleus size, i.e., number of atoms, n^*, or dimension l^*, and the nucleation barrier. The nearly *vertical thin downward line* corresponds to the atomic plasma, where the chemical potential is high and the nucleation barrier vanishes. The *horizontal gray arrow* indicates a possible role of the catalyst particle as a nucleation seed. The *inset* shows thermodynamic equilibrium line between the H_2 gas and the storage phase (CH). The *figure* is reproduced from the Ref. [86]

Role of catalyst

Although the previous work [86] showed the feasibility of the spillover process, the role of catalyst was not considered, and the focus was on the variation of the hydrogen binding to the receptor and its thermodynamic comparison with gaseous H_2. The first attempt toward this direction was made by the Cheng and coworkers [88, 89], they studied the dissociative chemisorptions of molecular hydrogen and desorption of atomic hydrogen on common catalyst Pt cluster. They carried out a very detailed study and found the possible sites for the adsorption of H_2 molecules. The dissociative H_2 adsorption was caused by the charge transfer from Pt to H_2 molecules via the overlap of 5*d* orbitals of Pt and $1\sigma^*$ orbital of H_2. They concluded that the number of adsorbed H_2 increases with the increasing size of the cluster. Furthermore, they show that the binding strengths are clearly coverage dependent and decrease with the increasing coverage. This would essentially imply that the available H energy states on Pt catalyst raise, which approximately represent the increase of the chemical potential μ_H in the absence of significant contribution from entropy. They find for the low coverage the adsorption

strengths are very large and at the saturation level are closer to the energies on fully covered Pt(111) surface [88, 89]. In contrast, the strength of H- binding to sp^2-carbon receptor is shown to increase with the greater coverage due to its clustering and CH-phase formation [86]. This analysis reconcile the weak binding of H to the bare substrate by emphasizing the role of nucleation of high-coverage CH-phase, which must be forming in the process of spillover on graphene-receptor, more favorable than H_2 molecule [86].

The key elements of spillover process are kinetics, relative energy states of the hydrogen in its (i) dihydrogen gas form, (ii) at the metal catalyst, and (iii) on the receptor-substrate. These elements are analyzed in detail by Singh et al. [90]. By means of the first principle calculations they explain the thermodynamics and kinetics of the spillover process. They show that it is energetically unfavorable for the spillover to occur on a pristine graphene surface, unless the C–H binding energy is significantly improved. This can be achieved by the presence of a phase of hydrogenated graphene, defects, and doping. They show details of hydrogen binding to the catalyst particle, which was modeled by Pd_4 cluster and serves as a gateway to the entire process. They showed the importance of the catalyst saturation for bringing the energy closer to the range required for the spillover. They combine all the pieces such as molecular dihydrogen gas phase, H dissolved on the catalyst, and H in the "storage phase." and presented a quantitative schematic of spillover as shown in Fig. 8. On the left, the blue line marks the energy of H in its molecular form with the additional broad (also blue) range is the chemical potential of H including the entropic contribution at different gas conditions. On the right side, a family of thin dark blue lines corresponds to the energies of H bound to graphene, which vary with the size and the configuration of the cluster island [86] and converge to the CH-phase energy. The mid-section pink block shows the computed range of energies of H at the catalyst. The first H_2 molecule dissociates and binds to the catalyst rather strongly, and therefore μ_H lies deep in this picture. However, the energies of the subsequent H_2 binding gradually decrease, raising the μ_H. For the spillover of an H to occur from the metal, the μ_H must exceed the CH state energy level shown by the gray line before the metal cluster saturates, i.e., becomes unable to further accept new H_2 molecules [90]. The catalyst plays an important role in bringing the μ_H into this range. Possible metal-hydride phase formation imposes an additional constraint on the μ_H. The former must lie above the μ_H of the receptor, to avoid formation of metal hydride before the spillover, assuming that the hydride phase would inhibit the catalytic activity. They validated this model by exploring through ab initio computations the gradual energy change of H on the catalyst and show that it fits between the energy on the receptor and as free gas. Comparing these μ_H values, they identified the range of chemical potential favorable for the spillover [90]. They explicitly show the role of catalyst saturation and binding strength of H on the receptor in bringing the μ_H in this desirable range. Furthermore, they also calculate the adsorption energy of the H on Pd(111) surface, for coverage from 0.25 to 1 ML, as shown by red block in Fig. 8. They found that the adsorption energy of 0.25 ML hydrogen was only slightly higher ($\sim$0.1 eV) than that in the Pd_4. Therefore, it was concluded from this study that with increasing cluster size the threshold of the spillover may decrease but not very significantly.

In addition, they also study the effect of different metal element catalysts on the spillover by carrying out

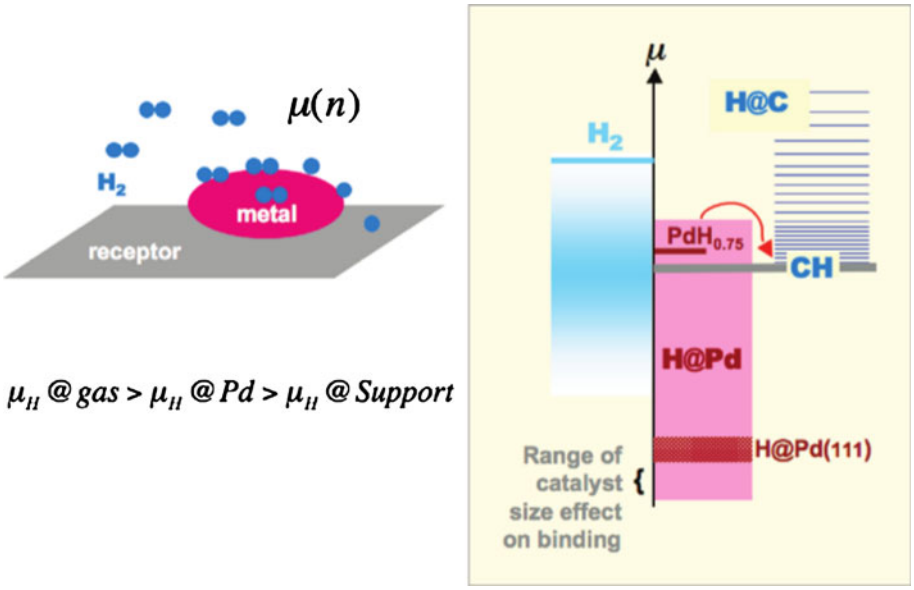

Fig. 8 *Left* schematics of spillover process in real space. *Right* model of spillover in energy space displays the relative energy (chemical potential) of H in different states. The *gray*, *dark-red*, and *blue lines* show the μ_H in fully hydrogenated graphene (CH), in metal hydride, and in the H_2 molecule, respectively. The *pink* and *dark-red blocks* show the range of energies of H at the catalyst and at the Pd(111) surface with the H coverage varying form 0.25 to 1 ML. The family of *thin dark-blue lines* corresponds to the energies of H bound to graphene. The *figure* is reproduced from the Ref. [90] (Color figure online)

hydrogenation of a Ni_4 cluster [90]. The effect of changing the metal from Pd to Ni essentially shifts in the threshold of the spillover, which occurs after adsorption on 7th H_2, compared with the Pd_4, where spillover becomes possible after adsorption of 6th H_2 molecule. This is due to the more diffused nature of Pd 4*d* orbital compared with the Ni 3*d* orbital. The overall catalytic activity of the Ni_4 cluster was found to be very similar to the Pd_4. This result would impact the economy of storage systems significantly as Ni is much cheaper metal than the Pd.

Kinetics

Singh et al. [90] extended their study to understand the kinetics of the spillover process. First, they assessed the likelihood of an H-atom to move from the catalyst to the pristine graphene substrate. This was tested by removing the H-atom from the saturated catalyst and placing it to the receptor. Upon relaxation, they found that H went back to the catalyst spontaneously, Fig. 9. When the removed hydrogen was placed farther away from the catalyst, it does not come back to catalyst even though the whole process became endothermic, highlighting again the difficulty of spillover on pristine graphene. On the other hand, when the removed H-atom is placed in the vicinity of a fully hydrogenated graphene phase, it was found that H did not come back to the catalyst, and the overall process becomes energetically favorable, making spillover possible on hydrogenated graphene [50, 91].

Next, Singh et al. [90] studied the motion of the H-atom from the catalyst to the receptor. The migration barrier for H to move from the metal to CH-phase was calculated by nudged elastic band method [92], Fig. 9, and found to be $E_s = 0.68$ eV. This barrier could be easily overcome even below the room temperature. They estimated the characteristic time τ of this step from standard rate theory [93] as $\tau^{-1} = (k_bT/h)\cdot\exp(-E_s/k_bT)$. At room temperature, the prefactor k_bT/h is 10^{13} s^{-1}, and $\tau \approx 30$ ms, which is reasonably fast [50]. Singh et al. [90] convincingly show the feasibility of spillover under the ambient condition both thermodynamically and kinetically.

In conclusion along with the catalyst saturation, the optimum C–H bonding has emerged as an important factor for the spillover. Therefore, any modification of the receptor that leads to an increase in this C–H interaction energy will potentially enhance the spillover. The incorporation of defects, curvature, and dopants are few routes to facilitate nucleation by improving the C–H binding. This has been demonstrated for graphene where the energy of hydrogenation changes drastically by Stone–Wales type of defects [94]. Lee et al. [95] have performed a first principles study of H spillover on IRMOF-1 and shown that the hole doping can substantially lower the energies as well as barriers to enable spillover at ambient conditions.

Conclusions and future perspective

We have reviewed the important contribution of first principle calculations on sorption materials and show how it has been instrumental in driving this technologically important area of research. The DFT has been extremely successful in predicting the adsorption energies for the Kubas type of binding of dihydrogen molecule in open transition metal atoms. The dihydrogen binding in alkali and alkaline earth metal requires more experiments to clear the doubts created by conflicting theoretical works. Indeed, the energy range for Kubas binding is very attractive for reversible ambient condition storage and has potential to provide an ideal storage media, which can easily meet the DOE targets. There remain open challenges to design such materials, such as metal atoms clustering apparently, turning out to be the strongest barrier. The key to the success lies in finding out materials, where metal atoms are integral part such as metallacarboranes. Hydrogen storage in graphitic materials via spillover has emerged a winner so far. The first principle-based calculations played an important role in explaining the thermodynamics and kinetics of this process and thereby removing the doubts on the experimental results. All the necessary ingredients to design an ambient condition sorbent system have been laid down by DFT calculations. This provides an ideal example,

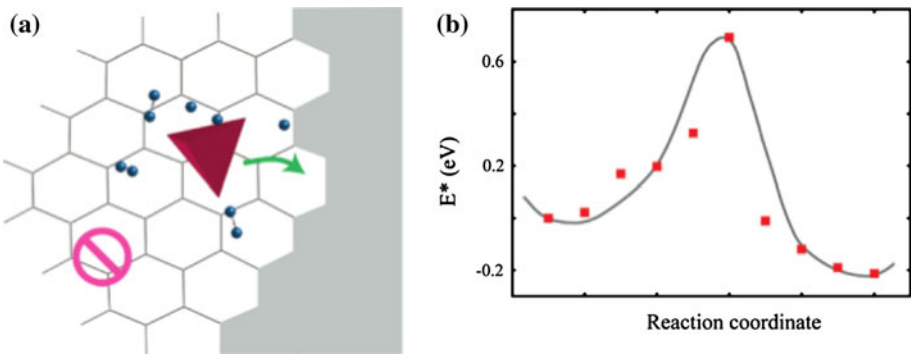

Fig. 9 **a** Structure of a relaxed cluster saturated with H, next to hydrogenated phase (*gray area*). **b** Plot of energies of intermediate images for the barrier calculation versus the reaction coordinate. The *figure* is reproduced from the Ref. [90]

where theory and experiments can go hand in hand in solving a very important problem.

Acknowledgements AKS thankfully acknowledge financial support from the Board of Research in Nuclear Sciences Grant No. 2011/37C/51/BRNS, and National Program on Micro and Smart Systems (NpMASS) PARC No. 1:22. Work at Rice University was initially supported by the Department of Energy Hydrogen Sorption Center of Excellence, and at later stage by the DOE BES Grant No. ER46598.

References

1. Crabtree GW, Dresselhaus MS, Buchanan MV (2004) Phys Today 39
2. Schlapbach L, Züttel A (2001) Nature 414:353
3. http://www1.eere.energy.gov/hydrogenandfuelcells/storage/pdfs/targets_onboard_hydro_storage_explanation.pdf (2009)
4. Dillon AC, Jones KM, Bekkedahl TA, Kiang CH, Bethune DS, Heben MJ (1997) Nature 386:377
5. Ding F, Lin Y, Krasnov PO, Yakobson BI (2007) J Chem Phys 127:164703
6. Ye Y, Ahn CC, Witham C et al (1999) Appl Phys Lett 74:2307
7. Liu C, Fan YY, Liu M, Cong HT, Cheng HM, Dresselhaus MS (1999) Science 286:1127
8. Yoon M, Yang S, Wang E, Zhang Z (2007) Nano Lett 7:2578
9. Pupysheva OV, Farajian AA, Yakobson BI (2008) Nano Lett 8:767
10. Sandrock G (1999) J Alloy Compd 293:877
11. Schüth F, Bogdanovi B, Felderhoff M (2004) Chem Commun 2249
12. Orimo S-i, Nakamori Y, Eliseo JR, Zuttel A, Jensen CM (2007) Chem Rev 107:4111
13. Rowsell JLC, Yaghi OM (2006) J Am Chem Soc 128:1304
14. Dinca M, Long JR (2008) Angew Chem Int Ed 47:6766
15. Kubas GJ (1988) J Acc Chem Res 21:120
16. Niu J, Rao BK, Jena P (1992) Phys Rev Lett 68:2277
17. Gagliardi L, Pyykkö P (2004) J Am Chem Soc 126:15014
18. Yildirim T, Ciraci S (2005) Phys Rev Lett 94:175501
19. Zhao Y, Kim Y-H, Dillon AC, Heben MJ, Zhang SB (2005) Phys Rev Lett 94:155504
20. Michael P (2001) J Organomet Chem 635:1
21. Gregory JK (2001) J Organomet Chem 635:37
22. Tast F, Malinowski N, Frank S, Heinebrodt M, Billas IML, Martin TP (1996) Phys Rev Lett 77:3529
23. Zhang Y, Dai H (2000) Appl Phys Lett 77:3015
24. Yildirim T, Íñiguez J, Ciraci S (2005) Phys Rev B 72:153403
25. Sun Q, Jena P, Wang Q, Marquez M (2006) J Am Chem Soc 128:9741
26. Kim Y-H, Zhao Y, Williamson A, Heben MJ, Zhang SB (2006) Phys Rev Lett 96:016102
27. Yoon M, Yang S, Hicke C, Wang E, Geohegan D, Zhang Z (2008) Phys Rev Lett 100:206806
28. Zhou W, Yildirim T, Durgun E, Ciraci S (2007) Phys Rev B 76:085434
29. Phillips AB, Shivaram BS (2008) Phys Rev Lett 100:105505
30. Sorokin PB, Lee H, Antipina LY, Singh AK, Yakobson BI (2011) Nano Lett 11:2660
31. Sun Q, Wang Q, Jena P, Kawazoe Y (2005) J Am Chem Soc 127:14582
32. Krasnov PO, Ding F, Singh AK, Yakobson BI (2007) J Phys Chem C 111:17977
33. Philipsen PHT, Baerends EJ (1996) Phys Rev B 54:5326
34. Cotton FA, Wilkinson G, Murillo CA, Bochmann M (1999) Advanced inorganic chemistry. Wiley-Interscience, New York
35. Hawthorne MF, Zink JI, Skelton JM et al (2004) Science 303:1849
36. Singh AK, Sadrzadeh A, Yakobson BI (2010) J Am Chem Soc 132:14126
37. Farha OK, Spokoyny AM, Mulfort KL, Hawthorne MF, Mirkin CA, Hupp JT (2007) J Am Chem Soc 129:12680
38. Spokoyny AM, Farha OK, Mulfort KL, Galli S, Hupp JT, Mirkin CA (2009) Small 5:1727
39. Hamaed A, Trudeau M, Antonelli DM (2008) J Am Chem Soc 130:6992
40. Dinca M, Dailly A, Liu Y, Brown CM, Neumann DA, Long JR (2006) J Am Chem Soc 128:16876
41. Hoang TKA, Webb MI, Mai HV et al (2010) J Am Chem Soc 132:11792
42. Vitillo JG, Regli L, Chavan S et al (2008) J Am Chem Soc 130:8386
43. Shevlin SA, Guo ZX (2008) J Phys Chem C 112:17456
44. Wang L, Lee K, Sun Y-Y et al (2009) ACS Nano 3:2995
45. Cha J, Lim S, Choi CH, Cha M-H, Park N (2009) Phys Rev Lett 103:216102
46. Bajdich M, Reboredo FA, Kent PRC (2010) Phys Rev B 82:081405
47. Sun YY, Lee K, Wang L et al (2010) Phys Rev B 82:073401
48. Kiran B, Kandalam AK, Jena P (2006) J Chem Phys 124:224703
49. Durgun E, Jang Y-R, Ciraci S (2007) Phys Rev B 76:073413
50. Lueking AD, Yang RT (2004) Appl Catal A 265:259
51. Li Y, Yang RT (2005) J Am Chem Soc 128:726
52. Zacharia R, Kim KY, Kibria AKMF, Nahm KS (2005) Chem Phys Lett 412:369
53. Kim B-J, Lee Y-S, Park S-J (2008) J Colloid Interface Sci 318:530
54. Conner WC, Pajonk GM, Teichner SJ (1986) Spillover of sorbed species. Academic Press, Orlando
55. Lachawiec AJ, Qi G, Yang RT (2005) Langmuir 21:11418
56. Lueking AD, Yang RT (2002) J Catal 206:165
57. Chen CH, Huang CC (2008) Microporous Mesoporous Mater 112:553
58. Yang FH, Yang RT (2002) Carbon 40:437
59. Anson A, Lafuente E, Urriolabeitia E et al (2006) J Phys Chem B 110:6643
60. Yoo E, Gao L, Komatsu T et al (2004) J Phys Chem B 108:18903
61. Kim HS, Lee H, Han KS et al (2005) J Phys Chem B 109:8983
62. Kim BJ, Lee YS, Park SJ (2008) Int J Hydrogen Energy 33:4112
63. Reddy ALM, Ramaprabhu S (2008) Int J Hydrogen Energy 33:1028
64. Wu H, Wexler D, Ranjbartoreh AR, Liu H, Wang G (2010) Int J Hydrogen Energy 35:6345
65. Lin KY, Tsai WT, Yang TJ J Power Sources
66. Back CK, Sandi G, Prakash J, Hranisavljevic J (2009) J Phys Chem B 110:16225
67. Lupu D, Biris AR, Misan I, Jianu A, Holzhuter G, Burkel E (2004) Int J Hydrogen Energy 29:97
68. Díaz E, León M, Ordóñez S (2010) Int J Hydrogen Energy 35:4576
69. Marella M, Tomaselli M (2006) Carbon 44:1404
70. Contescu CI, Brown CM, Liu Y, Bhat VV, Gallego NC (2009) J Phys Chem C 113:5886
71. Li Y, Yang RT (2007) J Phys Chem C 111:11086
72. Lachawiec AJ, DiRamondo TR, Yang RT (2008) Rev Sci Instrum 79:063906
73. Tsao CS, Liu Y, Li M et al (2010) J Phys Chem Lett 1:1569
74. Tsao CS, Tzeng YR, MS Yu et al (2010) J Phys Chem Lett 1:1060

75. Zielinski M, Wojcieszak R, Monteverdi S, Mercy M, Bettahar MM (2005) Catal Commun 6:777
76. Li Y, Yang RT, Liu Cj, Wang Z (2007) Ind Eng Chem Res 46:8277
77. Li Y, Yang RT (2006) J Am Chem Soc 128:8136
78. Stuckert N, Wang L, Yang RT (2010) Langmuir 26:11963
79. Miller MA, Wang CY, Merrill GN (2009) J Phys Chem C 113:3222
80. Zlotea C, Campesi R, Cuevas F et al (2010) J Am Chem Soc 132:2991
81. Proch S, Herrmannsdofer J, Kempe R et al (2008) Chem Eur J 14:8204
82. Li Y, Yang RT (2008) AIChE J 54:269
83. Wang L, Yang RT (2010) Catal Rev 52:411
84. Sofo J, Chaudhari A, Barber G (2007) Phys Rev B 75:4
85. Stojkovic D, Zhang P, Lammert P, Crespi V (2003) Phys Rev B 68:5
86. Lin Y, Ding F, Yakobson BI (2008) Phys Rev B 78:041402
87. Suri M, Dornfeld M, Ganz E (2009) J Chem Phys 131:174703
88. Zhou C, Wu J, Nie A, Forrey RC, Tachibana A, Cheng H (2007) J Phys Chem C 111:12773
89. Chen L, Cooper AC, Pez GP, Cheng H (2007) J Phys Chem C 111:5514
90. Singh AK, Ribas MA, Yakobson BI (2009) ACS Nano 3:1657
91. Sha X, Knippenberg MT, Cooper AC, Pez GP, Cheng H (2008) J Phys Chem C 112:17465
92. Jónsson H, Mills G, Jacobsen KW (1998) Nudged elastic band method for finding minimum energy paths of transitions. World Scientific, Singapore
93. Glasstone S, Laidler KJ, Eyring H (1941) The theory of rate processes. McGraw-Hill Book Co., New York
94. Duplock EJ, Scheffler M, Linda PJD (2004) Phys Rev Lett 92:225502
95. Lee K, Kim Y-H, Sun YY et al (2010) Phys Rev Lett 104:236101